Computational studies on the α- and β- Elimination Pathways for the Kinetics and Thermodynamics of the Gas-Phase Pyrolysis of Allyl Formates

Adejoro Isaiah Ajibade, Adeboye Omolara Olubunmi

Chemistry Department, University of Ibadan, Nigeria
Telephone: 08058584417; E-mail: moadeb5848@yahoo.com

Abstract: The study of α- and β-elimination pathways for the pyrolysis kinetics and thermodynamics of allyl formate was carried out in the gas-phase using Density Functional Theory (DFT with B3LYP at 6-311++G (2DF, 2P) in Spartan. The two pathways proceeded through a six-centered cyclic transition state. The result obtained for the [C_α-O, (43-46%) C_α-H_{11} and C_β-H_5 (9-10%)] bond lengthening character in a single step suggested that the reaction is concerted and asynchronous. The energy of formation for the α-elimination pathway that is elimination initiated from the formyl moiety is lower compare with the β-elimination pathway, elimination initiated from the allyl moiety. The activation parameters [E_a=178.59kJ/mol, log A=10.10 s^{-1} ΔH^*=172.79 kJ/mol ΔS^*=8.16J/mol.K and ΔG^*= 167.20kJ/mol] obtained for the α-elimination pathway are in good agreement with the experimental value than the values obtained for the β-elimination pathway.
[Adejoro Isaiah Ajibade, Adeboye Omolara Olubunmi. **Computational studies on the α- and β- Elimination Pathways for the Kinetics and Thermodynamics of the Gas-Phase Pyrolysis of Allyl Formates.** *Nat Sci* 2016;14(4):74-82]. ISSN 1545-0740 (print); ISSN 2375-7167 (online). http://www.sciencepub.net/nature. 9. doi:10.7537/marsnsj14041609.

Keywords: Allyl formates, pyrolysis, pathways, Elimination, DFT calculations

1. Introduction

The gas-phase pyrolysis of some alkyl formate has been reported to give formic acid and corresponding unsaturated alkenes as the only product. According to experimental reports (Markens and Eversole, 1931; Anderson and Rowley, 1943; Szarc and Taylor, 1953; Blades, 1954; Gordon *et al.,* 1957; Vernon and Waddington, 1969; Gil'burd and Moin. 1967; Blades and Sandhu, 1971; Hamon *et al.,* 1989) the mechanism of these reactions proceeds through a concerted six-centered cyclic transition state (Figure 1).

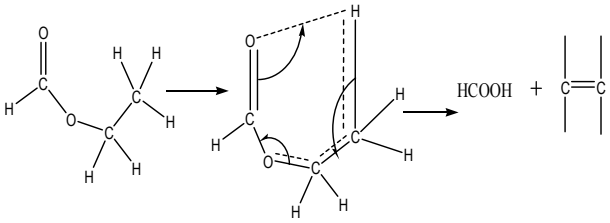

Figure 1. Mechanism of pyrolysis of alkyl formate

Allyl formate is an ester of formic acid which is obtained by replacing the phenyl π-system of a benzoyl formate (Vernon and Waddington, 1969) by a vinyl group when pyrolyzed in a static system produced propene and carbon (IV) oxide. The reaction was found to be homogeneous and follow a first order rate law. The results obtained were: energy of activation E_a = 43.15 ± 0.66 Kcal/mol (180.5 ± 2.9 kJ/mol), log A= 10.0 ± 0.2 and activation entropy ΔS^*= -14.6 ± 1.1e.u (-60.9 J/mol.K). These reaction was said to have proceeded through a [1, 5]-hydrogen shift (Figure 2) from the formyl hydrogen atom (Robinson and Holbrook, 1972).

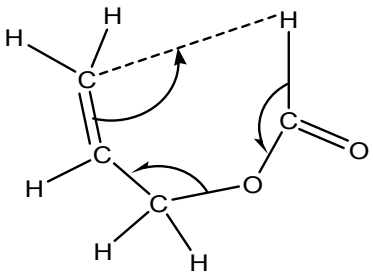

Figure 2. Mechanism of pyrolysis of allyl formate

Another work on the gas-phase pyrolysis of allyl formate to give carbon (IV) oxide and propene shows that log A=10.10 ± 0.3, ΔH^* = 174.00 kJ/mol, E_a = 179.91kJ/mol, K= 6.65 S^{-1} and ΔG^*= 167.74 kJ/mol. The recent theoretical calculation shows that the pyrolysis or thermal decomposition of allyl formate proceeds through a six-centered and a four-centered cyclic transition state to give carbon (IV) oxide and propene (Mora, *et al.,* 2013). However, from experimental and theoretical calculations obtained, it appears that there is a controversial problem of the minimum pathways leading to the gas-phase pyrolysis of allyl formats. Consequently, this work aimed at studying the α- and β-elimination pathways (elimination of hydrogen attached to the α-carbon of the formyl moiety and β-carbon of the allyl moiety) and the effect of these elimination pathways

on the kinetics and thermodynamic parameters using Spartan software with density functional theory method of calculations with Becky Lee Yang Parr number three at 6-311++G (2DF,2P) level.

2. Computational procedure

The mechanisms, kinetics and thermodynamics of the gas-phase pyrolysis of allyl formate have been examined using the densityfunctional theory (DFT) with B3LYP at 6-311++G(2DF, 2P) level using Spartan. Conformational search was done using molecular mechanics force field (MMFF) to obtain the most stable conformer (Warren, 2003). Geometry optimization was performed on the most stable conformer at the ground state, transition state and product to obtain the bond length, bond angle, dihedral angles and atomic charge distribution. Reaction path studies was carried out using α- H_{11}-C_1 and β- H_5- O_{12} as the reaction coordinates for allyl formats, here the internal coordinates were varied from its initial distance in the stable reactant form to its values in the product form. For allyl formate, the initial distance between H_{11} and C_1 is 3.331, and between H_5 – O_{12} is 4.478 Angstroms. The inter atomic distance was slowly altered throughout the reaction path calculation taking the value from 3.331 to 1.09 and 4.478 to 0.971 Angstroms its approximate value in the stable product molecule in 20 steps. Location and characterization of the transition state was done by subjecting the transition state structure to test in order to verify that the geometry corresponds to the transition state and that this correspond to the reactants and products. The tests are: there will be one imaginary IR value that will be in the range of 400-2000 cm^{-1} and the normal coordinates must correspond to the imaginary frequency which will connect the reactants and the product. The intrinsic reaction coordinate method was also used, kinetic and thermodynamic calculations were done using the data obtained from the geometric calculations on the reactants, transition state and products. The kinetic and thermodynamic parameters were obtained using the sum of the ground state energy (GSE) and the statistical mechanically calculated enthalpy to arrive at a closer approximation of the true energy of the molecule.

The enthalpy of a species will be defined as:

$H_i = GSE_i + H_i^{sm}$

Where the superscript 'sm' is the statistical mechanically calculated enthalpy. Substitute this into the initial definition of the heat of reaction we have:

$\Delta H_{rxn} = (GSE_{product} + H^{sm}{}_{product}) - (GSE_{reactant} + H^{sm}{}_{reactnt})$

Activation energy (Ea) was calculated according to the transition state theory for a unimolecular reaction at 698K (Warren and Ohlinger, 2009, 2010).

$E_a = \Delta H^* - RT$

The entropy of the reaction was calculated by taking the difference of product and reactant entropies that is

$$\Delta S_{reaction} = S_{product} - S_{reactants}$$

And $\Delta S_{activated} = S_{transition} - S_{reactant}$

The Gibbs free energy and Gibbs free energy of activation was calculated using the modified version of the heat of reaction equation. Knowing that The first order coefficient k(T) was calculated using transition state theory (TST) (Benson and O' Neal, 1970).

K' and h are the Boltzmann and Planck constants respectively.

Pre –exponential factor is given as $A = \frac{K_B T}{h} \exp\left[\frac{-\Delta S}{R}\right]$

The bond lengthening character was used to describe the extent of bond lengthening to show the rate determining step and to explain the concertedness and synchronicity of the reaction.

$G = H - TS$ and $\Delta G = \Delta H^* - T\Delta S$

Where ΔG^* is the Gibbs free energy change between the reactant and the transition state and

assuming that the transmission coefficient is unity as shown in the following equation $k(T) = \frac{K_B T}{h} \exp\left[\frac{-\Delta G^*}{RT}\right]$

Arrhenius rate was obtained using the rate equation (Wright, 2004)

$$k(T) = A \exp\left[\frac{-Ea}{RT}\right]$$

$$\text{Bond lengthening} = \frac{\text{TS bond length - GS bond length}}{\text{GS bond length}}$$

(Hamon *et al.,* 1989)

3. Results and Discussion

3.1 Conformational Search

Conformational search done using Molecular mechanics force field (MMFF) showed that allyl formats has five (5) different conformers with the most stable conformer having energy of -7.12kJ/mol (Figure 3).

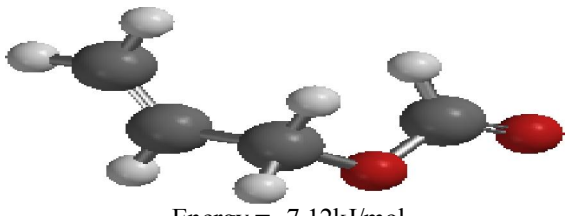

Energy = -7.12kJ/mol

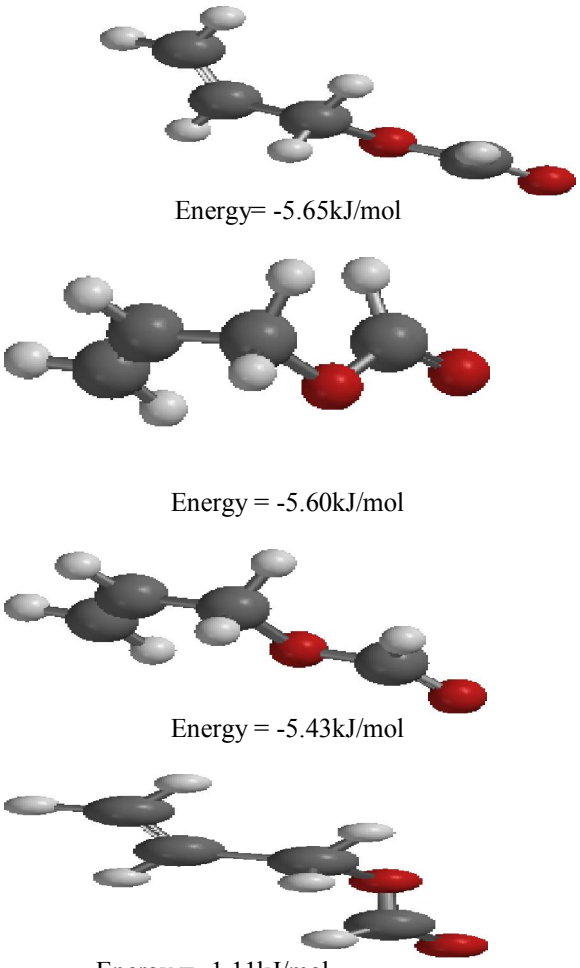

Figure 3. Conformers of Allyl Formate with their corresponding energy values.

3.1 Geometry optimization

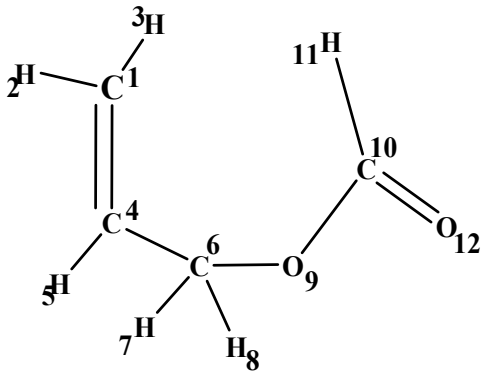

Figure 4. Sturcture of Allyl formate

Geometry optimization was performed on the structure of allyl formates (Figure 4) in the ground state, transition state and product to obtain the bond length, bond angles, dihedral angles and atomic charge distribution (Figure 5) for the α- and β-elimination series. The bond length (Table 1) observed between C_1- C_4 in the ground state for the α- and β-elimination series 1.326 changed to 1.381 and 1.322 respectively in the transition state but in the product form, it changed to 1.494 the expected bond length for a C-C single bond. It is observed that in the β-elimination series, the bond length between C_1- C_4 maintained the expected values for a C-C double bond in the GS, TS and product form (GS=1.326, TS=1.322 and Product=1.304). Considering the bond length between C_4- C_6, it is observed that the release of electron from C_6-O_9 and C_4-H_5 (points of cleavages) for both α- and β-elimination series makes the C_4- C_6 carbon-carbon single bond attained a carbon-carbon double bond character as shown in the values of the bond length in the transition state and product form (TS=1.381/1.373 and PRD=1.327/1.298 for α- and β-elimination series respectively. As shown in Table 1, for α- elimination series in the TS, the long stretch in the bond lengths between C_{10}-H_{11} (from 1.102 to 1.213) and C_6-O_9 (from1.444 to 2.068) are indications the cleavages occurs and between C_1-H_{11} from GS= no bond to TS=1.645 and finally to PRD=1.090 showed that a new bond is being formed. In the β-elimination series, the long stretch between C_4-H_5 (from1.085 to1.312) and C_6-O_9 (from 1.444 to 2.086) showed that cleavages also occurred at these points and the change in the bond length between O_{12}-H_5 from GS= no bond, TS=1.302 and PRD=0.971 are indications that a new bond has been formed.

Table 1 also showed the bond angles and the dihedral angles for the ground state, transition state and product, the variation in the values from ground state and transition state is as a result of distortion that occurred in the structures during the transitions process and this kind of distortion are necessary for intramolecular transfer of protons.

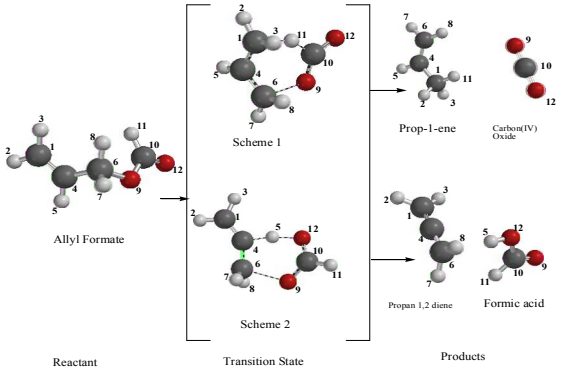

Figure 5. Optimized geometry of the reactant, transition state and products

Table1. Bond length, Bond angles and Dihedral angles for allyl formate (GS, TS and Products)

Bond Length (Å)		α-elimination	β-elimination
C_1–C_4	GS	1.326	1.326
	TS	1.381	1.322
	PRD	1.497	1.304
	Δd=TS-GS	+ 0.055	-0.004
C_4 –C_6	GS	1.495	1.495
	TS	1.381	1.373
	PRD	1.327	1.298
	Δd= TS-GS	-0.114	-0.122
C_6–O_9	GS	1.444	1.444
	TS	2.068	2.068
	PRD	-------	-------
	Δd= TS-GS	+0.624	+0.624
O_9 –C_{10}	GS	1.344	1.344
	TS	1.248	1.252
	PRD	1.159	1.193
	Δd= TS-GS	-0.096	-0.092
C_{10} –H_{11}	GS	1.102	1.102
	TS	1.213	1.107
	PRD	-------	1.103
	Δd= TS-GS	+0.111	+0.005
C_{10} –C_{12}	GS	1.193	1.193
	TS	1.212	1.278
	PRD	1.160	1.344
	Δd= TS-GS	+0.019	+0.085
C_4 –H_5	GS	1.085	1.085
	TS	1.312	1.312
	PRD	1.086	-------
	Δd= TS-GS	+0.227	+0.227
C_1 –H_{11}	GS	3.671	-
	TS	1.645	-
	PRD	1.090	-
	Δd= TS-GS	-2.026	-
O_{12} –H_5	GS	-	4.478
	TS	-	1.302
	PRD	-	0.971
	Δd= TS-GS		-3.176

Bond Angle (Å)		α-elimination	β-elimination
C_1-C_4– C_6	GS	124.05	124.05
	TS	116.90	143.13
	PRD	125.31	179.77
C_6-O_9– C_{10}	GS	117.43	117.43
	TS	113.81	113.77
	PRD	-	-
C_{10}-O_{12}– H_{11}	GS	113.13	113.13
	TS	109.79	117.13
	PRD	-	27.01
O_9-C_{10}– O_{12}	GS	122.78	122.78
	TS	135.93	124.96
	PRD	179.95	122.94

Dihedral Angle (Å)		α-elimination	β-elimination
C_1-C_4-C_6-O_9	GS	-129.26	-129.26
	TS	-65.18	-169.89
C_6-O_9-C_{10}-O_{12}	GS	-177.09	-177.09
	TS	-7.05	156.52
C_6-O_9-C_{10}-O_{11}	GS	3.65	3.65
	TS	-65.18	-22.59

3.2. Reaction path study

Reaction path calculations were performed on the optimized geometry of the allyl formate using α-H_{11}- C_1 and β-H_5- C_4 as the reaction coordinate (Bamkole, 2006). The internal coordinate was varied from its initial value in the stable reactant form to its value in the product molecule. According to previous report (Mclever and Kormonicki, 1971) instead of the energy to pass smoothly through a maximum, rose to a very high (219.46 and -43.23 kJ/mol for α and β-elimination respectively) value with a sudden drop in the geometry to a product with a drop in the heat of formation with the values approximately the same as the sum of the expected products, propylene and carbon (IV) oxide for α-H_{11} - C_1 and propan1, 2-diene and formic acid for β-H_5 - C_4. The result obtained showed that the pyrolysis of allyl formate can be initiated from the hydrogen that is attached to the α-carbon of the formyl moiety to give carbon (IV) oxide and propene and the hydrogen that is attached to the β-carbon of the allyl moiety to give propan-1, 2-diene and formic acid as shown Table 2 with the corresponding structures in Figure 6.

Table 2. Calculated Values for Energy of formation the Reaction Path Study for Allyl Formate

MOLECULES	Energy of Formation (kJ/mol) α- elimination	β-elimination
M0001	-274.45	-272.95
M0002	-273.83	-274.38
M0003	-273.05	-275.15
M0004	-272.15	-275.16
M0005	-271.17	-274.38
M0006	-269.87	-272.73
M0007	-267.66	-269.83
M0008	-266.44	-265.67
M0009	-261.76	-260.66
M0010	-254.63	-255.24
M0011	-245.65	-249.76
M0012	-233.93	-274.10
M0013	-214.85	-268.70
M0014	-182.84	-264.71
M0015	-138.05	-257.98
M0016	-86.52	-224.18
M0017	-30.10	-157.54
M0018	52.48	-95.29
M0019	219.46	-43.23
M0020	150.93	-127.48

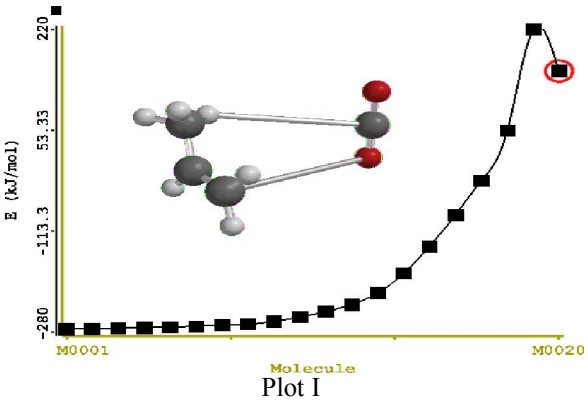

Plot I

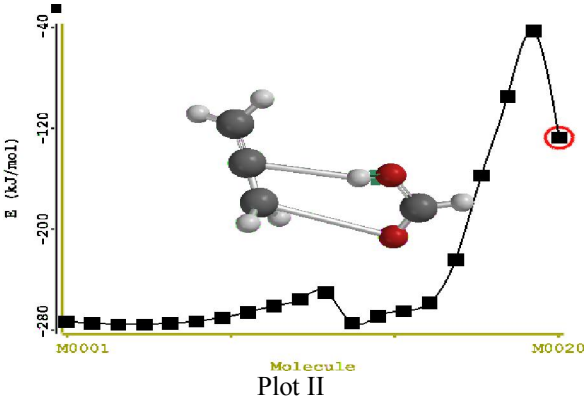

Plot II

Figure 6. Reaction path plot for allyl formate showing elimination of hydrogen at the α-carbon of the formyl moiety (Plot I) and β-carbon of the allyl moiety (Plot II)

3.3. Transition state

The transition state was characterized using two methods, the IR values obtained for the α and β-eliminations has only one imaginary IR values υ(i713 cm^{-1}), the main components of these stretching are C_1-H_{11} and C_{10}-H_{11} with intensity of 404.64 and υ(i1446cm^{-1}) with intensity 1062.67 are for C_4-H_5 and H_5-O_{12} stretching. The C_6-O_9 stretching is not present because the bond is virtually broken. The intrinsic reaction coordinate calculation converged and the plot (Figure 7) shows that the reaction is an exothermic reaction. Hammond postulate was used to further explain the intrinsic reaction coordinate calculation; the calculated energy of formation obtained showed that the transition state structure resembles the structure of the reactant because the energy of the transition state is closer to the reactant structure which is true for exothermic reactions and this also shows that the transition state structure is a later transition state (Anslyn and Dougherty, 2006; Hammond, 1955).

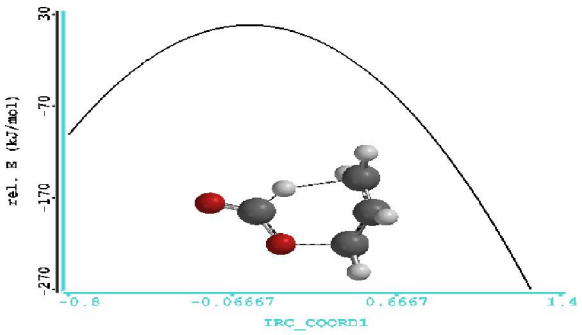

Figure 7. Intrinsic reaction coordinate plot

3.4 Mechanism of pyrolysis of allyl formates

The pyrolysis of allyl formate has been reported to proceeds through a four and a six-centered cyclic transition state initiated from the hydrogen that is attached to the α-carbon of the allyl moiety to give carbon (IV) oxide and propene as products and it was also reported that the four-membered cyclic transition state was less stable. However, the result obtained from this calculation showed that the pyrolysis of allyl formate could proceeds through a six-centered cyclic transition state initiated from the hydrogen that is attached to the α-carbon of the formyl moiety to give carbon (IV) oxide and propene and though a six-membered cyclic transition state initiated from the β-carbon of the allyl moiety to give propan-1, 2-diene and formic acid.

$C_4H_6O_2 \xrightarrow{\Delta} C_3H_6 + CO_2$
Allyl formate Propylene Carbon(IV) Oxide

$C_4H_6O_2 \xrightarrow{\Delta} C_3H_4 + CHOOH$
Allyl formate Propan-1, 2-diene Formic acid

These involves a six-membered cyclic transition state which proceeds through a C-H bond making, C-H (initiated from the hydrogen attached to the α-carbon of the formyl moiety) and C-O bond breaking on one part, a O-H bond making and C-H (initiated from the Hydrogen that is attached to the β-carbon of allyl moiety), C-O bond breaking on the other part, (Figure 8). In the transition state there is a stretch between C_{10} - H_{11} bond with bond length 1.213 against the bond length of 1.102 in the ground state for the α-elimination series. In the β-elimination series, the long stretch between C_4-H_5 (from1.085 to 1.312) and C_6-O_9 (from 1.444 to 2.086) showed that cleavages also occurred at these points and the change in the bond length between O_{12}-H_5 from GS=4.478, TS=1.302 and PRD=0.971 are indications that a new bond has been formed. Also, there is a stretch between C_6 - O_9, the bond length is 2.068 against bond length of 1.444 in the ground state

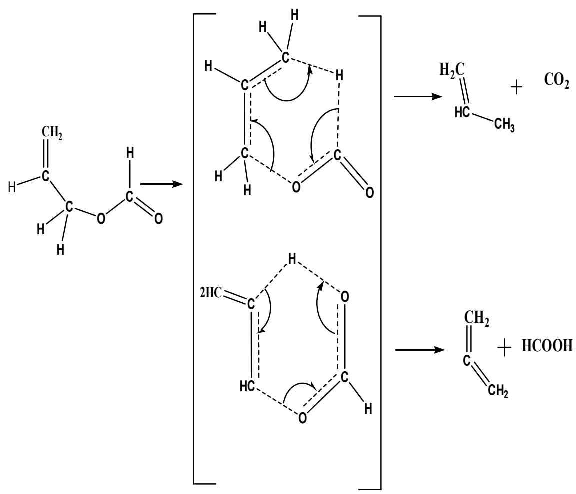

Figure 8. Reaction mechanisms of allyl formate showing elimination of hydrogen at the α-carbon of the formyl moiety and β-carbon of the allyl moeity

3.5 Atomic charges

The formal charge (Table 3) showed that α-H_{11} and β-H_5 has positive charge development (+0.21 and +0.46) while C_6 has negative charges (-0.292 and -0.630). The polarization of C_6-O_9 and C_1-H_{11} bonds causes positive charges on C_4 and C_{10} (+0.138 and +0.410) respectively and causes C_1 to become more negatively charged (-0.341) for the α-elimination series and the polarization of the O_{12}-H_5 and C_6-O_9 causes positive charges on C_4 and C_{10} (+0.343 and +0.192) to increase respectively (Figure 9).

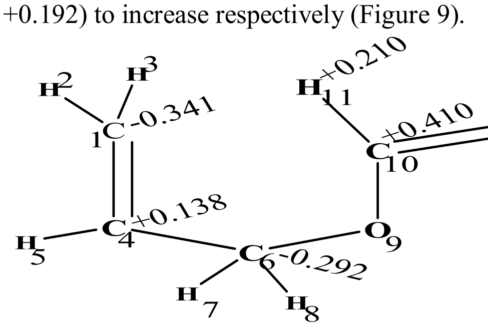

α-elimination series (formyl moiety)

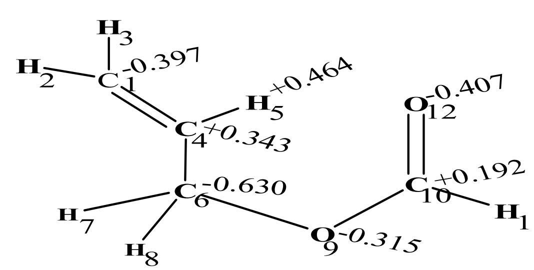

β-elimination series (allyl moiety)

Figure 9. Showing the distribution of atomic charges for α- and β-elimination series

Table 3. SELECTED ATOMIC CHARGES FOR ALLYL FORMATE [B3LYP/6-31++G(2DF,2P)]

ATOMS elimination		α- elimination	β-
C_1	GS	-0.426	-0.426
	TS	-0.340	-0.397
	PRD	-0.362	-0.482
	Δq =TS-GS	+0.086	+0.029
C_4	GS	+0.204	+0.204
	TS	+0.084	+0.343
	PRD	+0.138	+0.245
	Δq =TS-GS	-0.120	+0.139
C_6	GS	-0.260	-0.260
	TS	-0.293	-0.630
	PRD	-0.416	-0.330
	Δq =TS-GS	-0.033	-0.370
H_5	GS	-	+0.185
	TS	-	+0.464
	PRD	-	+0.295
	Δq =TS-GS	-	+0.279
C_{10}	GS	+0.212	+0.212
	TS	+0.192	+0.192
	PRD	+0.150	+0.150
	Δq =TS-GS	-0.020	-0.020
H_{11}	GS	+0.118	-
	TS	+0.214	-
	PRD	+0.096	-
	Δq =TS-GS		
O_{12}	GS		-0.341
	TS	-	-0.407
	PRD	-	-0.241
	Δq =TS-GS	-	-0.066

3.6 Calculation

The result obtained for kinetics and thermodynamic parameters (ΔH^* =172.79 & 190.90 kJ/mol, ΔS^* = 8.16 &13.16J/mol.K, ΔG^* = 167.20 & 181.83kJ/mol, E_a = 178.59 & 196.71kJ/mol, and log A = 13.58 S^{-1} for the α- and β- elimination series respectively compared favourably well with experimental results ((ΔH^* =174.00 kJ/mol, ΔG^* =167.74 kJ/mol, E_a = 179.91 kJ/mol and log A = 10.00 S^{-1} (Table 4). Negative Gibb's free energy (-103.46 and 130.93 kJ/mol) obtained showed that the reaction is spontaneous and the positive entropy of activation (8.16 and 13.16J/mol.K) suggest activation complexes with significant amount of bond cleavages to form two molecules (Anslyn and Dougherty, 2006). Negative values obtained for the enthalpy of reactions (-116.26 and -118.37 kJ/mol respectively) are indications that the reaction is an exothermic reaction, this confirmed with the intrinsic reaction coordinate plot (Figure 7) and the calculated energy of formation (Table 5) for the reactant, transition state and products obeyed Hammond's postulate (Figure 10) for exothermic reactions because the values obtained for the transition state is closer to that of the reactants which implies that the transition state structure resembles the structure of the reactants which provide a model for it.

Table 4. Kinetic And Thermodynamics Parameters For Allyl Formate At 698k [B3lyp/6-311++G (2df, 2p)]

Experimental values	calculated values		
PARAMETERS	**α-Elimination**	**β-Elimination**	
ΔH (kJ/mol)	-	-116.26	-118.37
ΔS J/mol.K	-	18.13	17.96
ΔG (kJ/mol)	-	-103.46	-130.93
ΔS^* J/mol.K	-	8.16	13.16
ΔH^* (kJ/mol)	174.00	172.79	190.90
ΔG^* (kJ/mol)	167.74	167.20	181.83
E_a (kJ/mol)	179.91	178.59	196.71
log A (s^{-1})	10.10	13.58	13.58
k (s^{-1})	1.16	1.68	1.37

The calculated bond lengthening character showed that the bond lengthened in the C_α- O bond is to a much greater extent (43-46%) than that of the C_α-H_{11} and C_β – H_5 bond (9-10%), the C_α- O bond dissociate in advance of C_α-H_{11} and C_β – H_5 to cause acceleration in the rate of the reaction. This also showed that the reaction is concerted because the bond cleavage and bond formation occurs in a single step and asynchronous because the dissociation of the C_α-O bond takes place before the formation of the C_1-H_{11} and O_{12} – H_5.

However, the activation parameters obtained for the β-elimination series is higher with corresponding low rate value compared with the α-elimination series.

Table 5. Energy of formation for allyl formate (kJ/mol)

α-Elimination		**β-Elimination**
GS	-804733.12	-804429.12
TS	-804557.25	-804247.68
PRD	-804851.25	-804538.75

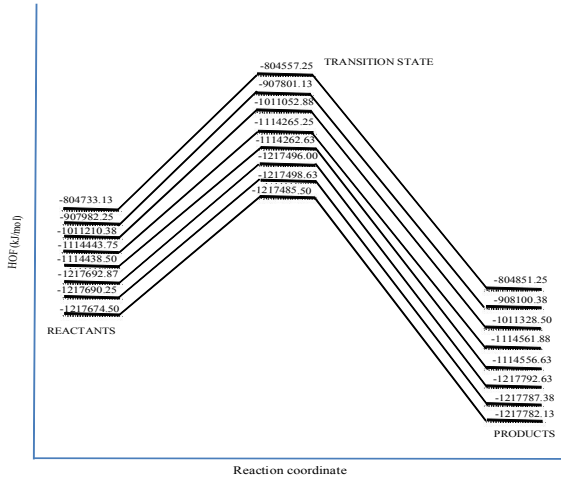

Figure 10. Energy diagram to depict Hammond's postulate

IR calculation obtained theoretically (Table 6) for the reactants, transition state and product for allyl formate for α- and β-elimination series are shown in (Fig.11a & 11b). The spectra for α-elimination in the transition and the product state (Fig) shows prominent absorption bands for $\upsilon(C{=}C_{str})$ at 1551cm^{-1}, $\upsilon(C{=}O_{str})$ 1798cm^{-1}, $\upsilon(C\text{-}H_{str\ sp^2})$ 1832cm^{-1} and $\upsilon(C\text{-}H_{str\ sp^3})$ 3135-3259cm^{-1} and for the β-elimination $\upsilon(C{=}O_{str})$ 1372-1389cm^{-1}, $\upsilon(C{=}O_{str})$ at 1662cm^{-1}, $\upsilon(C{=}C_{str})$ at 1808cm^{-1}, $\upsilon(C\text{-}H_{str\ carboxylic})$ at 2961cm^{-1}, $\upsilon(C\text{-}H_{str})$ at 3114 - 3217cm^{-1} and a sharp broad band that shows the appearance of υ(O-H) band at 3652cm^{-1}. These IR bands compared favourably well the experimental spectra (IR Absorption Table (*www.chem.ulca.edu/-webspectra/irtable.html*).

Table 6. Infra-red (cm^{-1})

REACTANT	**CALCULATED**	**EXPERIMENTAL**
$\upsilon(C\text{-}O_{str})$	1019, 1115	1200 -1180
$\upsilon(C{=}C_{str})$	1711	1600 -1500
$\upsilon(C{=}O_{str})$	1840	1750 -1700
$\upsilon(C\text{-}H_{str\ formyl})$	2958	2900 -2700
$\upsilon(C\text{-}H_{str})$	3033-3218	3100 -3010
PRODUCT		
α-elimination, β-elimination		
$\upsilon(C\text{-}O_{str})$	1145	1136
$\upsilon(C{=}O_{str})$	1798	1662, 1848
$\upsilon(C{=}C_{str})$	1551	2035, 1485
$\upsilon(C\text{-}H_{str\ sp^2})$	3135 -3259	3120 - 3206
$\upsilon(C\text{-}H_{str})$	1832	1808, 2961, 2965 (formic)
$\upsilon(O{=}H_{str})$	nil	3652

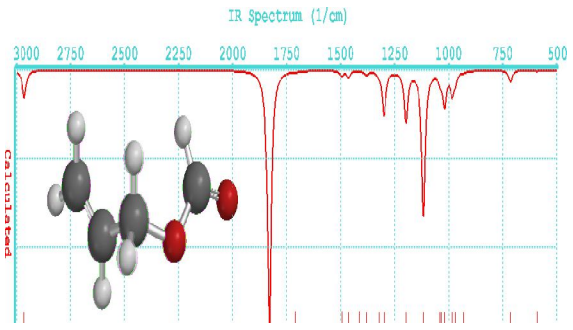

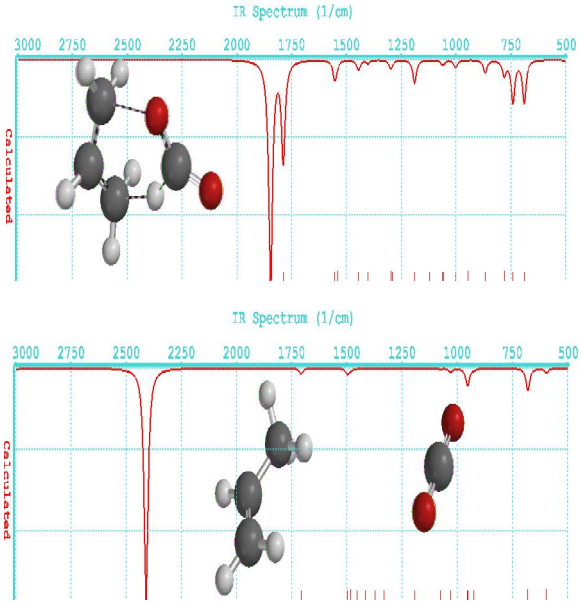

Fig 11a: IR spectra for α-elimination of allyl formate (GS, TS and PRD)

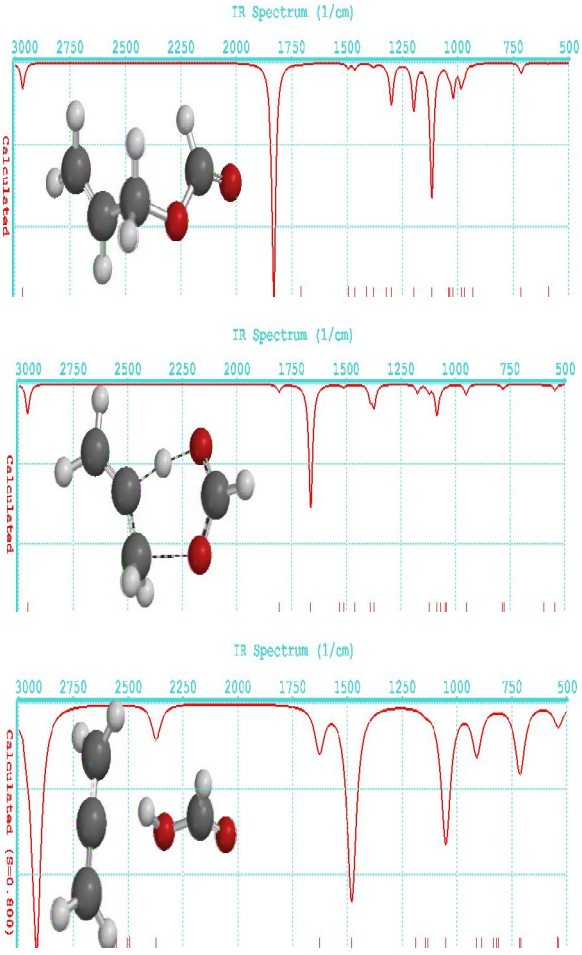

Fig 11b: IR spectra for β-elimination of allyl formate (GS, TS and PRD).

4. Conclusion

The α- and β-elimination pathway for the pyrolysis of the gas-phase pyrolysis of allyl formates was investigated using DFT with B3LYP at 6-311++G(2DF, 2P) level. Reaction path study calculation showed the the gas-phase pyrolysis could conviniently proceeds through the two pathways that is elimination initiated from the hydrogen that is attached to α-carbon of the formyl moeity and from the hydrogen that is attached to the β-carbon of the allyl moeity. However the energy of formation and other calculated kinetic and thermodynamic parameters for the elimination pathway from the hydrogen that is attached to α-carbon of the formyl moeity is lower compared with that of the β-carbon of the allyl moeity.

Acknowledgements:

Authors are greateful to the Department of Chemistry and the Postgraduate School University of Ibadan for creating a conducive enviroment to carry out this work.

Corresponding Author:
Adeboye, Omolara Olubunmi
c/o Dr. I.A. Adejoro
Department of Chemistry
University of Ibadan.
Telephone: 08058584417
E-mail: moadeb5848@yahoo.com

References

1. Makens, R. F., Eversole, W.C., Kinetics of the thermal decomposition of ethyl formate. J. Am. Chem. Soc. 61 1939; 3203-3206.
2. Blade, A.T. The Kinetics of pyrolysis of ethyl and isopropyl formates and acetates. Can. J. Chem. 32 1954; 366- 372.
3. Blades, A.T., Sandhu H. S. The Arrhenius factors for some six–center unimolecular reactions. Int. J. Chem. Kinet.III 1971;187- 193.
4. Gil'burd, M. M and Moin, F. B. Mass-spectrometric studies of fast high- temperature reactions II. Thermal decomposition of ethyl formate. Kinet. Katal. 8 1967; 261-264.
5. Anderson, R. B. and H. H. Rowley, Kinetics of the thermal decomposition of n-propyl and isopropyl formates, J. Phys Chem. 43 1943; 454-463.
6. Gordon, E., Price, S.J.W. Trotma- Dickenson A. F.. The pyrolysis of tert- butyl formate. J. Chem. Soc. 1957; 2813-2815.
7. Vernon, J. M. Waddington, D. Thermolysis of allylic formates. J. Chem. Commun II 1969; 623-624.

8. Szwarc, M. Watson Taylor, J. Pyrolyses of benzyl benzoate, acetate and formate. J. Chem. Phys. 211953; 1746-1749.
9. Hamon, L. Levaisalles, J. and. Pascal, Y.L A non-empirical 1,5 elimination transition structure for ethyl formate. Tetrahedron 45 1989; 1711-1722.
10. Robinson, P.J. and Holbrook, K. A. Unimolecular Reactions. John Wiley & Sons Ltd, 1972; 230.
11. Mora, J. R., Perez, D. C. Maldonado, A. Lorono, M. Cordova, T. and Chuchani, G. Theoretical study on thermal decomposition kinetics of allyl formates in the gas-phase. Elsevier-Computational and Theoretical Chemistry. 1019 2013; 48-54.
12. Warren Hehre, J. A Guide to Molecular Mechanics and Quantum Mechanical Chemical Calculations Irvine USA, 2003; 399.
13. Warren Hehre and Sean Ohlinger, Spartan '06 for Windows, Machintosh and Linux tutorial and user's guide. Wavefunction Inc. USA, 2006-2009.
14. Warren Hehre and Sean Ohlinger, Spartan '10 for Windows, Machintosh and Linux tutorial and user's guide. Wavefunction Inc. USA 2010.
15. Benson, S. W. and O' Neal Kinetic Data of Gas Phase Unimolecular Reactions. NSRDS- MBS 21 1970.
16. Wright, M. R. An Introduction to Chemical Kinetics. John. Wiley & Sons England, 2004; 100.
17. Bamkole, T. O. Calculation of the Arrhenius Parameters for the Pyrolysis of Some alkyl Vinyl Ether using Mopac. Journal of Applied Sciences 63 2006; 631 – 634.
18. Mclever, J. W. and Kormonicki, A. Rapid Geometry Optimization for Semi – Empirical Molecular Orbital Models. Chem. Phys. Letts. 10 1971; 303.
19. Anslyn, E.V. and Dougherty, D.A. Modern Physical Organic chemistry University Science Books. Wilsted and Taylor Publishing Services USA, 2006. *www.uscibooks.com*.
20. Hammond. G.S. J. Am. Chem. Soc. 77 1955; 334.
21. IR Absorption Table (*www.chem.ulca.edwebspectra/irtable.html*).

3/11/2016